Hawking radiation in dispersive theories, the two regimes

Stefano Finazzi*
INO-CNR BEC Center and Dipartimento di Fisica, Università di Trento, via Sommarive 14, 38123 Povo–Trento, Italy

Renaud Parentani†
Laboratoire de Physique Théorique, CNRS UMR 8627, Bât. 210, Université Paris-Sud 11, 91405 Orsay Cedex, France

(Dated: February 28, 2012)

We compute the black hole radiation spectrum in the presence of high frequency dispersion in a large set of situations. In all cases, the spectrum diverges like the inverse of the Killing frequency. When studying the low frequency spectrum we find only two regimes: an adiabatic one where the corrections with respect to the standard temperature are small, and an abrupt one regulated by dispersion which is well described using step functions. The transition from one regime to the other is governed by a single parameter which also governs the net redshift undergone by dispersive modes. These results can be used to characterize the quasi-particles spectrum of recent and future experiments aiming to detect the analogue Hawking radiation. They also apply to theories of quantum gravity that violate Lorentz invariance.

PACS numbers: 04.62.+v, 04.70.Dy, 03.75.Kk

I. INTRODUCTION

For long wavelengths, the propagation of sound waves in a moving fluid is analogous to that of light in a curved metric [1]. However, Hawking radiation issues from very short wavelength modes [2–5]. Therefore dispersion effects must be taken into account when computing the spectrum emitted by an acoustic black hole. When the dispersive scale ξ (the healing length in a Bose condensate) is much smaller than the surface gravity scale $1/\kappa$ which fixes the Hawking temperature $T_{\rm H} = \kappa/2\pi$ (in units where $\hbar = k_{\rm B} = c = 1$), it is now well understood that the spectrum is robust [6–17]. However the precise extension of this regime, and the spectral properties outside it are still poorly understood.

The aim of this paper is to remedy this situation. Doing so we shall complete Ref. [15] where we studied flow profiles with a local perturbation that strongly varies close to the horizon. In that paper we found two regimes: as long as the perturbation scale is larger than a certain critical length, the temperature is the standard one fixed by κ. For variations on shorter distances instead, the temperature is given by a spatial average over that critical length. Interestingly the latter is not simply given by the dispersive length ξ. Rather it scales as $\xi^{2/3}\,\kappa^{-1/3}$ for quartic dispersion.

To complete that analysis, we study the spectrum in simpler flows characterized by less parameters. We observe two well defined regimes. Firstly, when the flow is smooth and dispersion negligible, the spectrum slightly differs from the relativistic one. Secondly, there is an opposite regime of strong dispersion and steep horizon which is well described by using step-like profiles [18, 19]. With numerical techniques [14–16], we investigate the intermediate situations and show that there are no other regimes than these two, in agreement with [20]. We also show that the transition from one regime to other is governed by a single parameter which scales in the same way as the above mentioned critical distance. Interestingly, this parameter also fixes the (finite) redshift undergone by dispersive modes when scattered on a sonic horizon. For definiteness, we consider the phonon spectra in the context of atomic Bose condensates. Yet, our analysis applies to other superluminal dispersion relations, as well as subluminal ones, in virtue of the correspondence [17] between the various types of dispersion relations. It can therefore be used to explore the consequences on black hole thermodynamics [21] that arise from violations of Lorentz invariance found in certain theories of quantum gravity [22–25].

The paper is organized as follows. We first present the relevant parameters that govern the mode scattering on a sonic horizon. We then compute the low frequency limit of the emitted fluxes in step-like flow profiles. Finally, by numerically scanning a wide parameter space, we characterize the validity domains of both the Hawking and the step-like regimes. In Appendixes we present the basic concepts governing phonon fluxes, as well as the tools needed to compute these fluxes in step-like flows. We also show that our main results remain unchanged when considering a larger class of flows.

*Electronic address: finazzi@science.unitn.it
†Electronic address: renaud.parentani@th.u-psud.fr

II. RELEVANT CONCEPTS

A. Number of e-folds and critical frequency $\omega_{\max}$

We consider elongated condensates stationary flowing along the longitudinal direction x, and we assume that the transverse dimensions are small enough that phonon excitations are longitudinal. In the hydrodynamic regime, phonon propagation is governed by the d'Alembert equation in the metric [1, 26]

$$ds^2 = -c^2dt^2 + (dx - v\,dt)^2\ , \tag{1}$$

where the flow velocity v and the speed of sound c only depend on x. We assume that the condensate flows from right to left ($v < 0$), and that the sonic horizon (where $w = c + v$ crosses 0) is located at $x = 0$. When the gradient

$$\kappa \equiv \partial_x w|_{x=0} \tag{2}$$

is positive, one obtains an analogue black horizon. Indeed, in the near horizon region (NHR) where $w \sim \kappa x$ is a good approximation, the null geodesics are $x = x_0\, e^{\kappa(t-t_0)}$. Correspondingly, the wave vectors obey [5, 27]

$$k(t) = k_0\, e^{-\kappa(t-t_0)}. \tag{3}$$

These equations are the signatures of a (Killing) horizon. Notice that this exponential decay law is also found in an inflationary de Sitter space where the Hubble parameter H plays the role of κ. In that case, the number of e-folds $N = H(t - t_0)$ is used to quantify the duration of the inflationary period. The origin of this instructive correspondence is simple: in the NHR, the metric of Eq. (1) coincides with that of the flat sections of de Sitter in Lemaître coordinates, for details see Sec. 3.3 in [28].

When ignoring short distance dispersion, Eq. (3) implies that n_ω, the spectrum of upstream phonons spontaneously emitted from the horizon is Planckian with Hawking temperature $T_{\rm H} = \kappa/2\pi$, in units where $\hbar = k_B = 1$. When introducing dispersion, the spectrum n_ω is more complicated. To characterize its properties, we define the temperature function T_ω by

$$n_\omega \equiv \frac{1}{\exp(\omega/T_\omega) - 1}. \tag{4}$$

As such, T_ω is simply another way to express n_ω. It is particularly useful here because n_ω always diverges like $1/\omega$ for $\omega \to 0$ [14, 15, 18]. Hence the low frequency part of the spectrum is governed by the effective temperature

$$T_{\rm eff} \equiv \lim_{\omega\to 0} T_\omega = \lim_{\omega\to 0} \omega\, n_\omega. \tag{5}$$

We define the *Hawking regime* by situations where $T_{\rm eff}$ differs from $T_{\rm H}$ by less than 10%. We aim to determine the extension of this regime when introducing short distance dispersion.

In a stationary flowing atomic Bose condensate, the dispersion relation of phonons is given by

$$\begin{aligned}(\omega - vk)^2 &= \Omega^2(k) \\ &= c^2k^2 + \frac{\hbar^2k^4}{4m^2} = c^2k^2 + \frac{c^4k^4}{\Lambda^2},\end{aligned} \tag{6}$$

where ω is the conserved frequency $i\partial_t$, k the wave vector $-i\partial_x$, m the atom mass, and Λ the frequency associated with the healing length $\xi = \hbar/\sqrt{2}mc$ by $\Lambda = \sqrt{2}c/\xi$. This dispersion relation directly follows from the Bogoliubov-de Gennes equation [29], see Eq. (A6) in Appendix A, where more details can be found. Because of dispersion, phonons wave packets no longer follow null geodesics in the NHR [7, 12]. However, as long as the packet propagates in that region, Eq. (3) applies, irrespectively of the value of Λ/κ, and in fact irrespectively of the dispersion relation $\Omega(k)$. What is essential here is that the trajectories stay in the NHR only for a finite time. As a result, unlike what is found in de Sitter space, the accumulated red shift effect saturates at a finite value (when the asymptotic values of c and v are finite, which is the case we shall consider). To quantify this saturation, we use

$$e^{N_\omega} = r_\omega \equiv \frac{k_\omega^{(1),\rm as}}{k_\omega^{(2),\rm as}}, \tag{7}$$

where $k_\omega^{(1),\rm as}$ and $k_\omega^{(2),\rm as}$ are the asymptotic values of the in-going and out-going wave numbers, solutions of Eq. (6) with $\Omega < 0$, see Appendix A. These roots describe the negative frequency partner which is trapped in the supersonic region, on the left of the horizon. As we shall see, the number of e-folds N_ω, or its exponential r_ω, offers a simple description of the low frequency spectrum outside the Hawking regime. It is thus important to determine how it depends on the dispersive scale Λ and on the flow profile parameters.

To reduce the number of these parameters, we impose

$$\begin{aligned}c(x) &= c_0 + (1-q)w(x), \\ v(x) &= -c_0 + q\,w(x),\end{aligned} \tag{8}$$

where c_0 is the sound speed at the horizon. These equations specify how $w = c + v$ is shared between c and v. In the forthcoming numerical simulations, we shall use $q = 0.3$, which is a representative value of the generic case [14], and w given by [1]

$$\frac{w(x)}{c_0} = D\tanh\left(\frac{\kappa x}{c_0 D}\right). \tag{9}$$

The important quantity here introduced is D. It fixes the asymptotic value of w, but, more importantly, it also fixes

[1] In Appendix C, we consider more general profiles and observe that the main results are not significantly modified.

the extension of the NHR, i.e., the domain where $w \sim \kappa x$. This latter fact renders D a very relevant spectral parameter in the presence of dispersion [15, 17].

To compute r_ω of Eq. (7), we need to analyze the two roots of Eq. (6) with $\Omega < 0$. In the supersonic region, these roots merge in a point that corresponds to $x^{\rm tp}(\omega)$, the turning point of the trajectory at fixed ω [17]. Its location is fixed by solving $v_{\rm gr} = 0$, where the group velocity (in the horizon rest frame) is

$$v_{\rm gr} = \partial_k \omega = \partial_k(\Omega + vk). \tag{10}$$

Using Eq. (6), for $\omega \ll \Lambda$, one finds [8]

$$\frac{\kappa x^{\rm tp}(\omega)}{c_0} \approx -\left(\frac{\omega}{\Lambda}\right)^{2/3}. \tag{11}$$

For $\omega/\Lambda \to 0$, $x^{\rm tp}$ coincides with the horizon at $x = 0$, as expected from the behavior of the trajectories in the absence of dispersion. When ω increases, the turning point recedes to the left. We define the critical frequency $\omega_{\rm max}$ by the value of ω where $x^{\rm tp}(\omega)$ reaches $-\infty$. In the velocity flows of Eq. (9), one has $\omega_{\rm max} = \Lambda\, f(D, q)$ where f is a rather complicated function. For small values of D, which will be a relevant regime in the sequel, one gets

$$\omega_{\rm max} = \Lambda \left(\frac{2}{3} D\right)^{3/2} \left[1 + \frac{D}{2}\left(q - \frac{5}{6}\right) + O\left(D^2\right)\right]. \tag{12}$$

Using the asymptotic values of v and c, we can compute r_ω of Eq. (7), and relate it to $\omega_{\rm max}$. After a lengthy computation we obtain

$$r_\omega = \frac{3\sqrt{3}}{2}\frac{\omega_{\rm max}}{\omega}\left[1 + \frac{D}{6} - \frac{1}{3\sqrt{3}}\left(1 + \frac{D}{2}\right)\frac{\omega}{\omega_{\rm max}} + O\left(D^2\right) + O\left(\frac{\omega^2}{\omega_{\rm max}^2}\right)\right]. \tag{13}$$

For frequencies $\omega/\omega_{\rm max} \ll 1$ and small values of D, quite remarkably, r_ω depends only on $\omega_{\rm max}/\omega$.

At this point we remind the reader that in dispersive theories it was observed that $\omega_{\rm max}$ governs the first order deviations from the Hawking spectrum [13–16]. Since the two negative roots $k_\omega^{(i)}$, associated with the negative norm mode, no longer exist for $\omega > \omega_{\rm max}$, $\omega_{\rm max}$ acts as a cutoff above which there is no radiation. However, it is more subtle to understand why $\omega_{\rm max}$ also determines the low frequency ($\omega \ll \omega_{\rm max}$) properties of the spectrum. A detailed analysis [17] of the connection formula governing the scattering on the sonic horizon confirms that the first deviations from the Hawking spectrum are governed by the particular combination of Λ and D entering in $\omega_{\rm max}$. From Eq. (13) we learn that the same combination fixes the total redshift when D is small. As a result, we shall see that the transition from the Hawking regime to the other one can be meaningfully characterized by r_ω for $\omega = T_{\rm eff}$ of Eq. (5).

B. Fluxes for step-like profiles

When ignoring greybody factors, the spectral properties of n_ω are analytically known in the Hawking regime which is found in the dispersionless limit ($\Lambda \to \infty$, fixed κ). In the opposite limit of infinite surface gravity ($\kappa \to \infty$, fixed Λ), the spectral properties can be analytically computed [18–20]. In particular, the low frequency effective temperature $T_{\rm eff}$ of Eq. (5) is well defined. We call it $T_{\rm step}$ and we refer to this case as the *step-like regime*.

Before determining the extension of this domain, we generalize the treatment of the above references so as to work with condensate flows where both v and c have a jump at the sonic horizon. We focus on the low-frequency behavior of n_ω, the spectrum emitted in the subsonic region, and n_ω^v, the spectrum of left movers with respect to the atoms, see Eq. (A10). In the step-like regime, unlike what is found in the Hawking regime, the spectra of both right and left movers are predicted by the same techniques and should be treated on equal footing. In fact, whereas the spectrum of left-going particles is not well defined for gravitational black holes as there is no asymptotic region inside the horizon, it is perfectly well defined for acoustic black holes. Moreover the mode mixing of left and right movers has been observed in gravity waves experiments [30] and could be observed in the future in Bose–Einstein condensates. In Appendixes A and B we give a summary of the concepts needed to compute these two occupation numbers. Here we present only the main results.

In the low frequency limit, we obtain

$$n_\omega^{\rm step} = \frac{\Lambda}{\omega}\left(\frac{D}{2}\right)^{3/2}\left[1 - \frac{D}{2}\left(q + \frac{1}{2}\right) + O\left(D^2\right)\right] + Cst. \tag{14}$$

Using Eqs. (5) and (12), the effective temperature reads

$$T_{\rm step} = \frac{3\sqrt{3}}{8}\,\omega_{\rm max}\left[1 - \left(q - \frac{1}{6}\right)D + O\left(D^2\right)\right]. \tag{15}$$

This simple equation establishes the relevance of $\omega_{\rm max}$ in the step-like regime. In particular it establishes that $n_\omega \propto D^{3/2}$ as $D \to 0$. This non-trivial result is relevant for experiments in optical fibers and glasses where $D \lesssim 10^{-3}$. It is also interesting to express $n_\omega^{\rm step}$ in terms of r_ω of Eq. (7):

$$n_\omega^{\rm step} = \frac{r_\omega}{4}\left[1 - qD + O\left(D^2\right)\right]. \tag{16}$$

Hence, for small values of D, using Eq. (B18), we get another simple equation:

$$n_\omega^{\rm step} \approx \frac{r_\omega\,|v_u|}{4c_0}, \tag{17}$$

where v_u is the fluid velocity in the upstream region. We notice that $n_\omega^{\rm step}$ factorizes into r_ω and v_u, depending on

quantities which are respectively defined in the supersonic and subsonic region only.

Operating in a similar way, we obtain the number of left-going particles

$$n_\omega^{v,\,\mathrm{step}} = \sqrt{2}\left(q-\frac{1}{2}\right)^2 \frac{\Lambda}{\omega}\, D^{7/2} \times \left[1-\frac{D}{2}\left(q+\frac{1}{2}\right)+O\left(D^2\right)\right]+Cst. \quad (18)$$

In analogy with Eq. (5), we define T^v_{eff} the effective temperature of left movers. In the step-like regime, we get

$$T^v_{\mathrm{step}} = \frac{3\sqrt{3}}{2}\,\omega_{\max}\, D^2 \left(q-\frac{1}{2}\right)^2 \left[1-\left(q-\frac{1}{6}\right)D\right] + O\left(D^4\right). \quad (19)$$

Note that T^v_{step} vanishes quadratically when $q = 1/2$. This is reminiscent of what was numerically noticed in [14] for continuous profiles. In that case it was found that the mixing between right- and left-going modes was minimum for this value. For a step-like profile, the first non-vanishing term is

$$n_\omega^{v,\,\mathrm{step}} = \frac{D^{11/2}}{1152\sqrt{2}}\left[1+\frac{D}{2}\right]\frac{\Lambda}{\omega}+O\left(D^{13/2}\right). \quad (20)$$

Finally, since both n^v_ω and n_ω diverge in the same way for $\omega \to 0$, it is convenient to compute their ratio

$$R_{\mathrm{eff}} \equiv \lim_{\omega\to 0}\left(\frac{n^v_\omega}{n_\omega}\right). \quad (21)$$

For step-like profiles, using Eqs. (14) and (20), one gets

$$R_{\mathrm{step}} = 4\left(q-\frac{1}{2}\right)^2 D^2 + O\left(D^4\right). \quad (22)$$

From this ratio, we learn that n^v_ω is highly suppressed in optical fibers since $D \ll 1$, and that it is not directly related to r_ω of Eq. (7), unlike what is found for the right movers in Eq. (16). In that case indeed, for $D \ll 1$, both T_{step} and r_ω have the same dependence on Λ, D and q.

In the next section, we determine the validity domain of these formulas. It is rather clear that the above expressions should be valid in the limit of infinite surface gravity: $\kappa/\Lambda \to \infty$ at fixed D. Rather surprisingly, we shall see that they are also valid for very small κ/Λ when $D \to 0$.

III. THE EXTENSION OF THE TWO REGIMES

A. The Hawking regime

We start with the extension of the Hawking regime. This has been already studied and it is rather well understood. Using numerical techniques [14], it was found that the first order deviations from the Hawking spectrum are mainly controlled by $\omega_{\max}/\kappa$. They thus scale as $\Lambda D^{3/2}$, see Eq. (12). In fact, it was found that these deviations hardly depend on Λ/κ when working at fixed $\omega_{\max}/\kappa$. Using the same code, we now clarify these observations and also investigate the spectral properties further away from the Hawking regime. To these ends, we plot in Fig. 1 the ratio $T_{\mathrm{eff}}/T_{\mathrm{H}}$ in the two-dimensional parameter space defined by $\omega_{\max}/\kappa$ and Λ/κ. We use logarithmic scales to see more easily the scaling properties. The value of the parameter q has been chosen to be 0.3, to avoid the peculiar cases of $q = 1/2$ or $q = 1/6$, where some contribution cancels, as can be seen from the expressions given in Sec. II B.

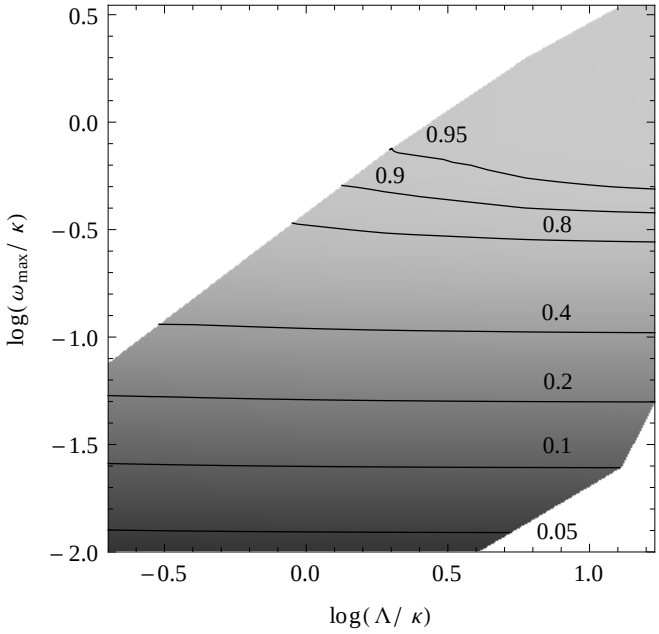

FIG. 1: $T_{\mathrm{eff}}/T_{\mathrm{H}}$ as a function of Λ/κ and $\omega_{\max}/\kappa$ in logarithmic scales. The parameter q of Eq. (8) is 0.3. Solid lines are locii of constant $T_{\mathrm{eff}}/T_{\mathrm{H}}$. One clearly sees that the departures from the Hawking regime are essentially governed by $\omega_{\max}/\kappa$. Roughly speaking, one leaves the Hawking regime (i.e., T_{eff} and T_{H} differ by 10%) for $\omega_{\max}/\kappa \lesssim 0.4$, irrespectively of the value of Λ/κ. *N.B.* The upper white area is due to the fact that we restrict our analysis to $D < 1$, whereas the lower one is due to our incapacity of numerically obtaining n_ω for $D \lesssim 0.02$.

For $\omega_{\max}/\kappa \gtrsim 1$, we see that $T_{\mathrm{eff}}/T_{\mathrm{H}} \to 1$ in a manner that hardly depends on Λ/κ. The region $\omega_{\max}/\kappa \gtrsim 1$ therefore characterizes the situations where Hawking's result is robust. For $\omega_{\max}/\kappa \ll 1$, the effective temperature T_{eff}, strongly differs from T_{H}. However it still hardly depends on the dispersive scale Λ/κ. Therefore $\omega_{\max}/\kappa$ is the most relevant spectral parameter in the *entire plane*. This important lesson is corroborated by the results presented in the following subsection.

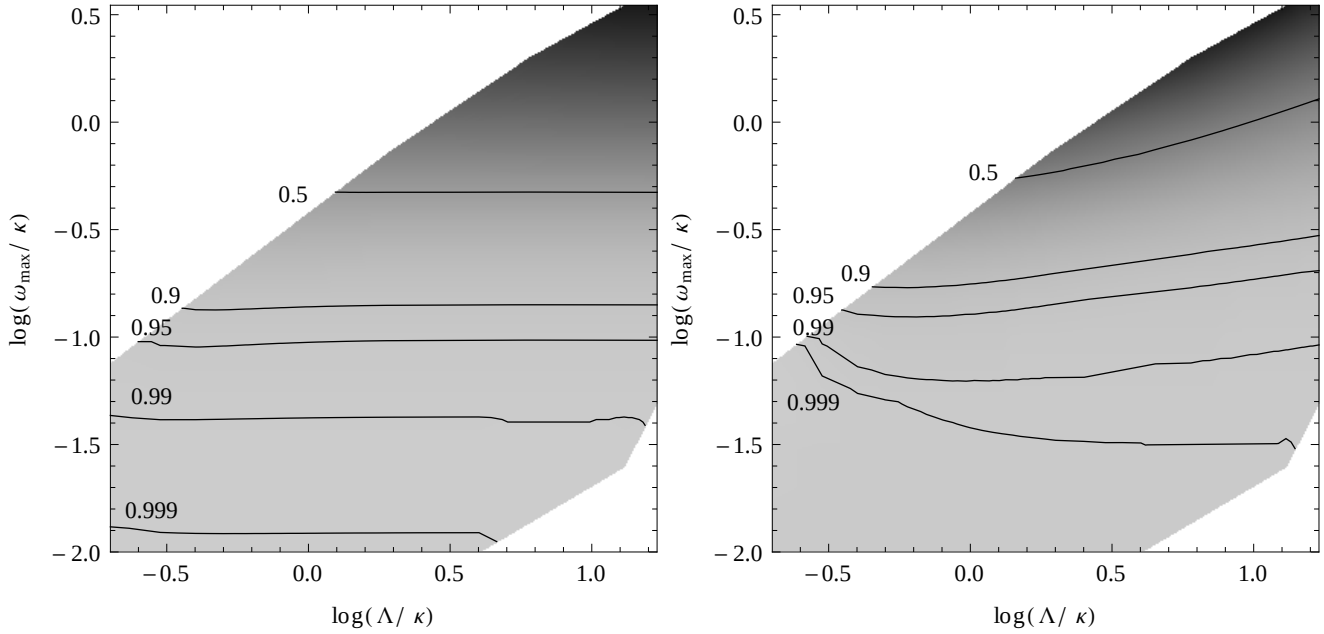

FIG. 2: The temperature ratios $T_{\rm eff}/T_{\rm step}$ (left panel) and $T^v_{\rm eff}/T^v_{\rm step}$ (right panel) as a function of Λ/κ and $\omega_{\rm max}/\kappa$ for the same situations as in Fig. 1, where $T_{\rm step}$ and $T^v_{\rm step}$ are obtained from Eqs. (B16) and (B17). The departures from the step-like regime are essentially governed by $\omega_{\rm max}/\kappa$. Roughly speaking, one leaves this regime for $\omega_{\rm max}/\kappa \gtrsim 0.1$, irrespectively of the value of Λ/κ.

B. The step-like regime

In a manner strictly similar to what we have just done for the Hawking regime, we study the validity domain of the expressions obtained in Sec. II B. In Fig. 2 we plot $T_{\rm eff}/T_{\rm step}$ (left panel) and $T^v_{\rm eff}/T^v_{\rm step}$ (right panel) for the same situations as in Fig. 1. The first lesson from Fig. 2 is that these two ratios behave in a very similar manner. Secondly, when $\omega_{\rm max}/\kappa \lesssim 0.1$, we see that the effective temperatures $T_{\rm eff}$ and $T^v_{\rm eff}$ obtained with the regular profiles of Eq. (9) are in excellent agreement with $T_{\rm step}$ and $T^v_{\rm step}$ obtained in Sec. II B. In addition, we learn that this agreement is reached in a manner that hardly depends on Λ/κ. Therefore, quite remarkably, the step-like regime is found even when scale separation is achieved, i.e., for $\Lambda/\kappa \gg 1$, when D is small enough that $\omega_{\rm max}/\kappa \lesssim 0.1$.

To complete our analysis, in Fig. 3 we plot the ratio $R_{\rm eff}$ of Eq. (21). We note that the lines of constant $R_{\rm eff}$ almost coincide with the lines of constant D (slope 2/3, dashed lines). Hence $R_{\rm eff}$ scales as D^2. This scaling is in perfect agreement with the step-like prediction of Eq. (22). This is a further confirmation of the applicability of step-like techniques in a wide region of parameters. However, unlike $T_{\rm eff}$ and $T^v_{\rm eff}$ that are well approximated by using a step-like profile only for $\omega_{\rm max}/\kappa \lesssim 0.1$, their ratio behaves as D^2 in the whole plane. This means that $R_{\rm eff}$ scales in the same way in the Hawking and in the step-like regime.

We also emphasize that $R_{\rm eff}$ is maximal for large values of D. This is also rather unexpected as it was believed that the coupling between right and left sectors should be a sub-dominant effect for smooth profiles. When adding high frequency dispersion to a 2D conformally invariant massless field [6, 7], this is indeed the case [13]. However when using the quasi-particle wave equation of some condensed matter model, there is no reason to believe that this should still be the case. (From Figs. 11 and 12 of [14] it is clear that in Bose–Einstein condensates, the spectrum n^v_ω of left movers is generically large.)

IV. SUMMARY AND INTERPRETATION

To summarize the results, we schematically illustrate in Fig. 4 the validity regions of the two regimes. The region where the temperature $T_{\rm eff}$ differs from $T_{\rm H}$ by less than 10% is shaded in dark gray, whereas that approximatively governed by a step-like profile is shaded in light gray. We re-emphasize that the expressions obtained using a step-like profile provide very good approximations not only where κ/Λ is large (right lower corner), but in general when $\omega_{\rm max}/\kappa$ is small, independently of the value of κ/Λ.

In Fig. 4, we see that the white area from $0.1 \lesssim \omega_{\rm max}/\kappa \lesssim 0.4$ is not covered by either approximation. To characterize the effective temperature in this transitory regime, we use the *average* temperature $T_{\rm av}$ of [15]. It is obtained by taking the spatial average of the gradient of

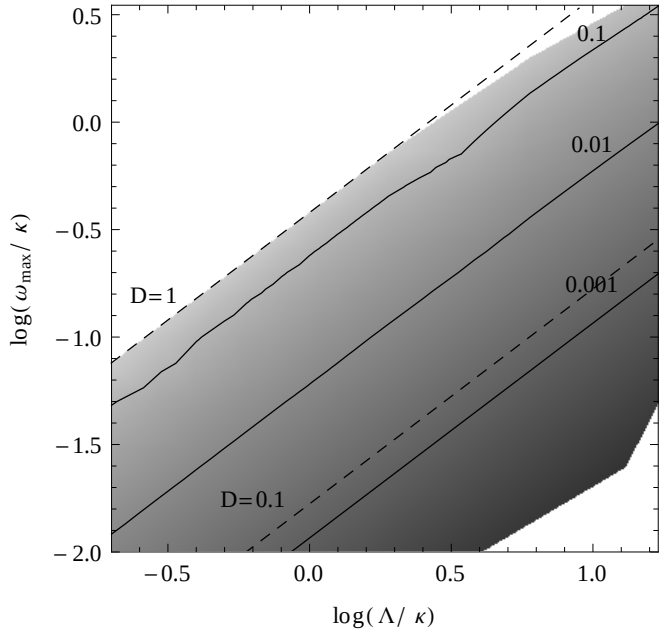

FIG. 3: $R_{\rm eff}$ defined in Eq. (21) as a function of Λ/κ and $\omega_{\rm max}/\kappa$ for the same situations as in Fig. 1. Solid lines give the various values of this ratio, whereas the dashed straight lines with slope 2/3 are locii of constant D, see Eq. (12). Clearly, $R_{\rm eff}$ depends only on D.

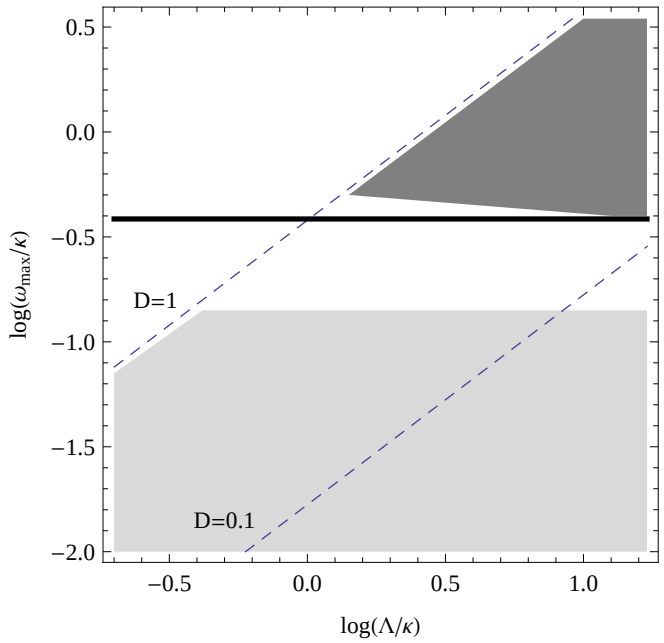

FIG. 4: In dark gray we denote the validity region (defined by 10% difference in temperature) of the Hawking regime, and in light gray that of the step-like regime. The thick horizontal line is the threshold value of Eq. (26). The dashed straight lines are locii of constant D. It is clear that $\omega_{\rm max}/\kappa$ governs the extension of the two domains, and the transition between them.

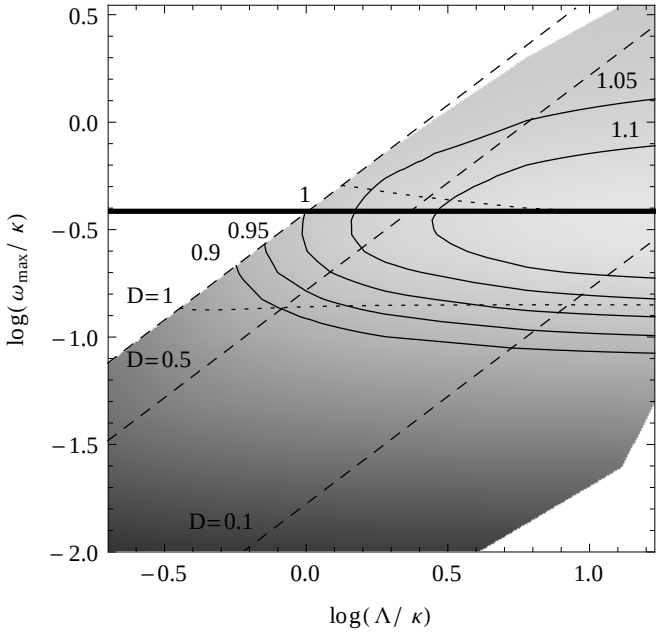

FIG. 5: $T_{\rm eff}/T_{\rm av}$ as a function of Λ/κ and $\omega_{\rm max}/\kappa$ in logarithmic scale for the same profiles as in Fig. 1, where $T_{\rm av}$ is given by Eqs. (23) and (24). Solid lines are locii of constant $T_{\rm eff}/T_{\rm av}$. The other lines are as in Fig. 4.

$w = c + v$ over a given length d_ξ

$$T_{\rm av} \equiv \int_{-d_\xi/2}^{d_\xi/2} dx\, \frac{dw}{dx} = \frac{2w(d_\xi/2)}{d_\xi}. \tag{23}$$

The critical length was found to be

$$d_\xi = d\, c_0 \left(\kappa\Lambda^2\right)^{-1/3}, \tag{24}$$

where d is approximatively equal to $2^{2/3}$. When the extension of the NHR where $w \sim \kappa x$ is larger than d_ξ, $T_{\rm av}$ agrees with the Hawking temperature $T_{\rm H}$.

Transposing these notions to the present context, the boundary of the region where the Hawking regime ceases to be valid should thus be given by the condition that the extension of the NHR of Eq. (9) equals d_ξ:

$$2\frac{Dc_0}{\kappa} = d_\xi. \tag{25}$$

Using Eqs. (24) and (12), this condition fixes the threshold value of $\omega_{\rm max}/\kappa$ to be

$$\frac{\omega_{\rm max}}{\kappa}|_{\rm threshold} = \frac{2}{3\sqrt{3}}. \tag{26}$$

In Fig. 4, the black solid line represents this value. In accord with the analysis of [15, 17], it precisely lies where the Hawking regime ceases to be valid.

To be more precise and more quantitative, we now compare $T_{\rm av}$ with the effective temperature $T_{\rm eff}$. Their ratio is plotted in Fig. 5. As expected, $T_{\rm av}$ is very close to

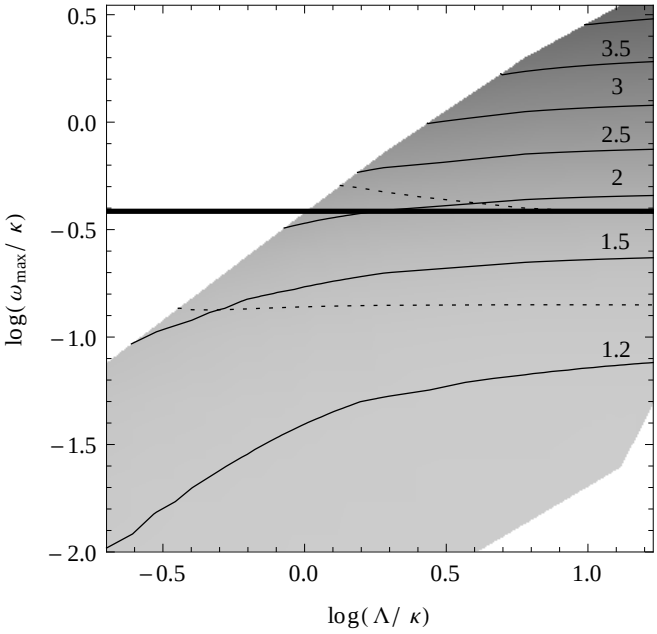

FIG. 6: The number of e-folds of Eq. (7) evaluated for $\omega = T_{\rm eff}$ as a function of Λ/κ and $\omega_{\rm max}/\kappa$ for the same profiles as in Fig. 1. The dotted lines bound the regions of validity (with 10% errors) of the Hawking regime (upper line) and the step-like regime (lower line). The thick line is the threshold value of Eq. (26).

$T_{\rm eff}$ when D and Λ/κ are large. When $D \ll 1$, $T_{\rm av}$ is a bit less accurate in reproducing $T_{\rm eff}$ than $T_{\rm H}$, even if $\omega_{\rm max}/\kappa$ is large. However, $T_{\rm av}$ gives a rather good approximation of $T_{\rm eff}$ in a much broader region than $T_{\rm H}$. Within an error of 10%, the region covered by $T_{\rm av}$ extends down to $\log_{10}\omega_{\rm max}/\kappa \approx -1$. The average temperature $T_{\rm av}$ therefore correctly describes $T_{\rm eff}$ in the transition region where both $T_{\rm H}$ and $T_{\rm step}$ fail to do so.

Now, what is the physical meaning of Eq. (26)? Using Eq. (13), we see that $\omega_{\rm max}$ is proportional to $\omega\, r_\omega$. To be able to define a threshold value for the number of e-folds $N_\omega = \ln r_\omega$, we need to pick a frequency ω. In the sequel, we work with $\omega = T_{\rm eff}$ since $T_{\rm eff}$ characterizes the actual spectrum n_ω for $\omega \to 0$. When $\omega_{\rm max} < \omega_{\rm max}|_{\rm threshold}$, we see in Fig. 6 that $N_{\omega=T_{\rm eff}}$ is almost constant and slightly larger than 1. It has to be noticed that it does *not* go to 0 as $D \to 0$ when working with $\omega = T_{\rm eff}$. When $\omega_{\rm max}$ is above the threshold, $N_{T_{\rm eff}}$ increases exponentially as a function $\omega_{\rm max}/\kappa$. We therefore conclude that the number of e-folds evaluated at the typical frequency $T_{\rm eff}$ provides an extremely simple way to characterize the validity domains of the two regimes. That is, the Hawking regime starts above $N_{T_{\rm eff}} \sim 2$, whereas the step-like analysis provides reliable results when $N_{T_{\rm eff}}$ is smaller than 1.4.

To conclude this paper we first underline that our results, which have been obtained using the superluminal quartic dispersion of Eq. (6), also apply to other types of superluminal relations, and to subluminal ones, in virtue of the correspondence between these cases [17].

Secondly, we point out that our analysis can be easily used to characterize the outcome of recent and future experimental investigations aiming to detect the analogue Hawking effect. Indeed the knowledge of Λ/κ and $\omega_{\rm max}/\kappa$ suffices to determine in which regime one will find the (low frequency part of the) quasi-particle spectrum. For instance, a step-like analysis should be appropriate for experiments in optical fibers or glasses since these are characterized by a small parameter D, typically of order $\lesssim 10^{-3}$ [31, 32], in spite of the fact that $\Lambda/\kappa \gg 1$. Thus, in these cases, a precise knowledge of the surface gravity is not required to predict the spectrum. On the contrary, for experiments in Bose–Einstein condensates [33] or in water [30], the spectrum will be essentially governed by the surface gravity because D is of the order of unity, and $\Lambda/\kappa > 1$.

Thirdly, our analysis can be used to characterize the Hawking radiation in theories of quantum gravity [22–25] which contain violations of Lorentz invariance at very high energies. In particular, Fig. 1 indicates that the black hole temperature should no longer be given by the surface gravity when κ/Λ becomes larger than 1. Understanding the possible consequences of this on black hole thermodynamics [21] is an interesting and challenging question.

Acknowledgments

SF thanks I. Carusotto for helpful suggestions and A. Recati for explanations about [18]. RP wishes to thank U. Leonhardt for conversations (in winter 2004) on Hawking radiation in optical fibers during which he realized that the parameter D and the number of e-folds must play a crucial role. We both thank A. Coutant for a careful reading of this work.

Appendix A: Mode analysis and scattering matrix

We present the main concepts that characterize the scattering of phonons in atomic Bose condensates in stationary flows containing one sonic horizon. We follow the treatment of Ref. [14] where more details can be found.

In non homogeneous condensates, phonon elementary excitations are appropriately described by *relative* density perturbations:

$$\hat\Psi = \Psi_0(1+\hat\phi), \tag{A1}$$

where $\hat\Psi$ is the atom field operator, and Ψ_0 the condensate. The dynamics of $\hat\phi$ is determined by the Bogoliubov–de Gennes equation [29]:

$$i\partial_t\hat\phi = \left[T_\rho - iv\partial_x + mc^2\right]\hat\phi + mc^2\hat\phi^\dagger, \tag{A2}$$

where $\hbar = 1$, c is the x-dependent speed of sound

$$c^2(x) \equiv \frac{g(x)\rho_0(x)}{m}, \tag{A3}$$

$\rho_0(x) = |\Psi_0(x)|^2$ is the mean density of condensed atoms, and $g(x)$ is the effective coupling constant among atoms. These functions play no role in the sequel: only $c(x)$ and $v(x)$ matter. The kinetic operator that acts on $\hat\phi$ is

$$T_\rho = -\frac{1}{2m}\, v\partial_x \frac{1}{v}\partial_x. \tag{A4}$$

In stationary situations, $\hat\phi$ can be expanded in frequency eigenmodes

$$\begin{aligned}\hat\phi &= \int d\omega \left[e^{-i\omega t}\hat\phi_\omega(x) + e^{+i\omega t}\hat\varphi_\omega(x)^\dagger\right] \\ &= \int d\omega \sum_\alpha \left[e^{-i\omega t}\phi^\alpha_\omega(x)\hat a^\alpha_\omega + e^{+i\omega t}(\varphi^\alpha_\omega(x))^*\hat a^{\alpha\dagger}_\omega\right], \end{aligned}\tag{A5}$$

where the discrete sum over α takes into account the number of modes at fixed ω. Inserting Eq. (A5) in Eq. (A2) yields the following system

$$\begin{aligned}\left[(\omega + iv\partial_x) - T_\rho - mc^2\right]\phi^\alpha_\omega(x) &= mc^2\varphi^\alpha_\omega(x),\\ \left[-(\omega + iv\partial_x) - T_\rho - mc^2\right]\varphi^\alpha_\omega(x) &= mc^2\phi^\alpha_\omega(x).\end{aligned}\tag{A6}$$

In backgrounds containing one sonic horizon, there are two or three modes depending on whether ω is larger or smaller than $\omega_{\max}$ of Eq. (12). More precisely the ω component of the field operator reads

$$\hat\phi_\omega = \phi^u_\omega \hat a^u_\omega + \phi^v_\omega \hat a^v_\omega + \theta(\omega_{\max}-\omega)\varphi^*_{-\omega}\hat a^\dagger_{-\omega}. \tag{A7}$$

For $\omega > 0$, the modes ϕ^u_ω and ϕ^v_ω have positive norm, they describe, respectively, propagating right-u and left-v moving waves with respect to the condensed atoms and they are associated with the usual real roots of Eq. (6), see Fig. 7. On the contrary, $(\varphi_{-\omega})^*$ has a negative norm. It is associated with the extra roots that exist in supersonic flows for $\omega < \omega_{\max}$, and describes phonons that are trapped inside the horizon ($x < 0$) in the supersonic region.

In our infinite condensates, the above modes become superpositions of plane waves both in the left and right asymptotic regions of Eq. (A7). We can thus construct without ambiguity the in- and out-mode bases. The in (out) modes are such that each of them contains only one asymptotic branch with group velocity directed towards (away from) the horizon. For $\omega > \omega_{\max}$, there exist only two positive norm modes, and therefore in and out modes are linearly related by a trivial (elastic) 2×2 transformation. Instead, when $\omega < \omega_{\max}$, the in and out modes mix with each other in a nontrivial way by a 3×3 Bogoliubov transformation [14]

$$\begin{aligned}\phi^{u,\mathrm{in}}_\omega &= \alpha_\omega \phi^{u,\mathrm{out}}_\omega + \beta_{-\omega}\left(\varphi^{\mathrm{out}}_{-\omega}\right)^* + \tilde A_\omega \phi^{v,\mathrm{out}}_\omega,\\ (\varphi^{\mathrm{in}}_{-\omega})^* &= \beta_\omega \phi^{u,\mathrm{out}}_\omega + \alpha_{-\omega}\left(\varphi^{\mathrm{out}}_{-\omega}\right)^* + \tilde B_\omega \phi^{v,\mathrm{out}}_\omega,\\ \phi^{v,\mathrm{in}}_\omega &= A_\omega \phi^{u,\mathrm{out}}_\omega + B_\omega\left(\varphi^{\mathrm{out}}_{-\omega}\right)^* + \alpha^v_\omega \phi^{v,\mathrm{out}}_\omega.\end{aligned}\tag{A8}$$

The standard mode normalization yields relations such as (from the first equation)

$$|\alpha_\omega|^2 - |\beta_{-\omega}|^2 + |\tilde A_\omega|^2 = 1. \tag{A9}$$

When the initial state is vacuum, the final mean occupation numbers are given by

$$\begin{aligned} n_\omega = |\beta_\omega|^2, \quad n^v_\omega = |\tilde B_\omega|^2,\\ n_{-\omega} = n_\omega + n^v_\omega.\end{aligned}\tag{A10}$$

The third equation, which gives the number of negative frequency phonons, follows from energy conservation which imposes that each pair spontaneously produced should have no energy. In the standard analysis without dispersion, n_ω is Planckian and describes the Hawking effect [5]. In that case, for massless conformally invariant fields, the number n^v_ω of left moving phonons identically vanishes because the coupling between u and v modes is zero. Adding high frequency dispersion to that case, one finds $n^v_\omega \ll n_\omega$. Hence the scattering of this dispersive field on a sonic horizon basically consists of a more general and slightly modified version of the standard Hawking effect, as long as $\omega_{\max} \gtrsim \kappa$. For larger values of κ, and for non-conformally invariant fields, deviations with respect to the relativistic case can be large, but the structure of Eq. (A8) and the meaning of its coefficients remain unchanged [14, 18, 19].

Appendix B: Step-like profiles

We extend the computation of the Bogoliubov coefficients given in [18, 19] to step-like profiles where the velocity is different on the upstream and downstream sides of the horizon. That is we consider profiles given by

$$v(x) = v_u\,\theta(x) + v_d\,\theta(-x), \tag{B1}$$
$$c(x) = c_u\,\theta(x) + c_d\,\theta(-x). \tag{B2}$$

For these profiles, Eq. (A6) can be solved separately in the upstream ($x > 0$) and downstream ($x < 0$) regions by Fourier transform:

$$\phi_i(x) = \sqrt{\frac{\partial k_i}{\partial\omega}}\,\frac{e^{-i\omega t + ik_i x}}{\sqrt{4\pi\rho_i}}\,u_i, \tag{B3}$$
$$\varphi_i(x) = \sqrt{\frac{\partial k_i}{\partial\omega}}\,\frac{e^{-i\omega t + ik_i x}}{\sqrt{4\pi\rho_i}}\,v_i, \tag{B4}$$

where the index i stands for u (upstream) when $x > 0$ and d (downstream) when $x < 0$. (For the sake of conciseness we have omitted the indexes α and ω). The normalization factor has been chosen such that

$$u_i^2 - v_i^2 = 1, \tag{B5}$$

where u_i, v_i are chosen real. On each side Eq. (A6) gives

$$\begin{aligned}\left[(\omega - v_i\,k_i) - \frac{k_i^2}{2m} - mc_i^2\right]u_i &= mc^2\,v_i,\\ \left[-(\omega - v_i\,k_i) - \frac{k_i^2}{2m} - mc_i^2\right]u_i &= mc^2\,u_i.\end{aligned}\tag{B6}$$

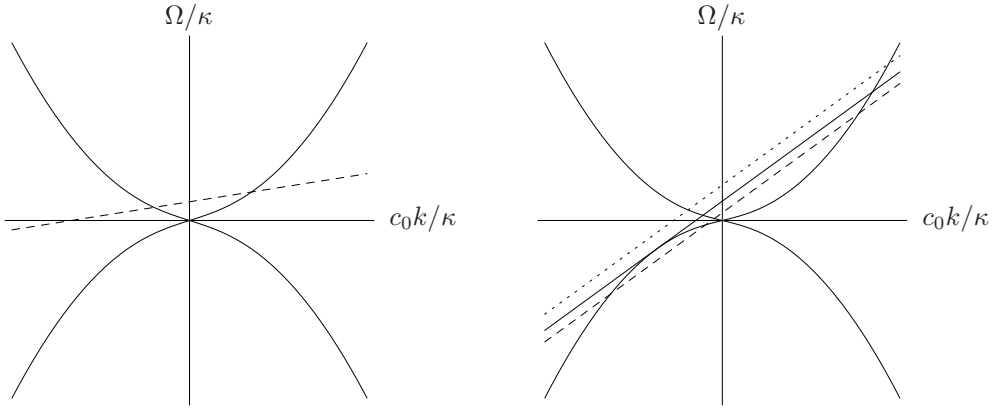

FIG. 7: Graphical solution of the dispersion relation (6) for subsonic (left panel) and supersonic flow (right panel). Solid curves: $\pm\Omega(k)/\kappa$. In subsonic flows, for $\omega > 0$ the dashed line $(\omega - vk)/\kappa$ crosses twice the dispersion relation with $\Omega > 0$. In supersonic flows, two extra roots exist in the left lower quadrant for $\omega < \omega_{\rm max}$ (dashed line). For $\omega = \omega_{\rm max}$ the solid line is tangent to $\Omega(k)$, and for $\omega > \omega_{\rm max}$ (dotted line) these real roots no longer exist.

Since the dispersion relation is quartic, we obtain four roots $k(\omega)$. Hence, for a given frequency ω, the general solution can be written on either side as superposition of four momentum eigenmodes. Notice that k are all real in the downstream supersonic region, whereas two are real and the other two complex conjugated in the upstream region.

In order to obtain globally defined solutions we need to match the two sets of modes. Firstly, the solutions $\phi_{\omega,i}(x)$ and $\varphi_{\omega,i}(x)$ must be continuous at the horizon, that is

$$\phi_u^+ = \phi_d^-\,, \quad \varphi_u^+ = \varphi_d^-\,, \tag{B7}$$

where the superscript $\pm$ denotes the limit of the function for $x \to 0^{\pm}$, respectively. Secondly, the matching conditions for the derivatives of ϕ and φ can be obtained by integrating the system (A6) in a small neighborhood $[-\varepsilon, \varepsilon]$ of the horizon and taking the limit for $\epsilon \to 0$. To characterize this limit, it is useful to write T_ρ of Eq. (A4) as

$$T_\rho = -\frac{1}{2m}\partial_x^2 + \frac{1}{2m}\left[\partial_x \log(v(x))\right]\partial_x. \tag{B8}$$

For our profiles, the second term gives

$$\begin{aligned}\partial_x \log(v(x)) &= \partial_x\left[\log(v_u)\,\theta(x) + \log(v_d)\,\theta(-x)\right]\\ &= \log(v_u)\,\delta(x) - \log(v_d)\,\delta(-x) = \log\left(\frac{v_u}{v_d}\right)\delta(x).\end{aligned} \tag{B9}$$

The non-trivial terms of the first equation of Eq. (A6) are

$$\begin{aligned}i\int_{-\varepsilon}^{\varepsilon} dx\, v\,\partial_x\phi + \frac{1}{2m}\int_{-\varepsilon}^{\varepsilon} dx\,\partial_x^2\phi\\ - \frac{1}{2m}\log\left(\frac{v_u}{v_d}\right)\int_{-\varepsilon}^{\varepsilon} dx\,\delta(x)\,\partial_x\phi = 0.\end{aligned} \tag{B10}$$

Since ϕ is continuous at $x = 0$, its derivative can have at most a finite jump at $x = 0$. Therefore, the integrand in the first integral has a finite jump at $x = 0$, such that, when taking the limit $\varepsilon \to 0$, this term vanishes. The second integral can be directly computed because its integrand is the derivative of $\partial_x\phi$. It gives the jump in the first derivative of the field ϕ:

$$\int_{-\varepsilon}^{\varepsilon} dx\,\partial_x^2\phi = \partial_x\phi_u^+ - \partial_x\phi_d^-\,. \tag{B11}$$

Finally, the last integral gives

$$\begin{aligned}\log\left(\frac{v_u}{v_d}\right)\int_{-\varepsilon}^{\varepsilon} dx\,\delta(x)\,\partial_x\phi\\ = \frac{1}{2}\log\left(\frac{v_u}{v_d}\right)\left[\partial_x\phi_u^+ + \partial_x\phi_d^-\right].\end{aligned} \tag{B12}$$

Taking into account these last equations, the matching condition of the first derivative is

$$\left[1 - \frac{1}{2}\log\left(\frac{v_u}{v_d}\right)\right]\partial_x\phi_u^+ = \left[1 + \frac{1}{2}\log\left(\frac{v_u}{v_d}\right)\right]\partial_x\phi_d^-\,. \tag{B13}$$

From the second equation of (A6), one finds an identical condition for $\partial_x\varphi$. In brief, we get

$$\phi_u^+ = \eta\,\phi_d^-\,, \quad \varphi_u^+ = \eta\,\varphi_d^-\,, \tag{B14}$$

where

$$\eta \equiv \frac{2 - \log(v_d/v_u)}{2 - \log(v_u/v_d)}. \tag{B15}$$

Using Eqs. (B7) and (B14), for $\omega < \omega_{\rm max}$, one can determine the three globally defined solutions that are *asymptotically bounded* and that appear in Eq. (A7). From them we can extract the nine coefficients of Eq. (A8). The computation is rather tedious, but completely analogous to what was performed in [18, 19]. Below we only give the dominant term in the limit $\omega \to 0$ of two Bogoliubov coefficients β_ω and $\tilde{B}_\omega$ which determine n_ω and n_ω^v. We obtain

$$\beta_\omega = \sqrt{\frac{\Lambda}{\omega}} \times \frac{\sqrt{c_u}}{c_0} \sqrt{\frac{v_d}{v_u}} \sqrt{\frac{c_u+v_u}{c_u-v_u}} \frac{\left(v_d^2-c_d^2\right)^{3/4}}{c_u^2-c_d^2+c_u(v_u-v_d/\eta)} \left[\sqrt{c_u^2-v_u^2} - i\,\frac{v_d v_u - \eta\, c_d^2}{\sqrt{v_d^2-c_d^2}}\right], \tag{B16}$$

$$\tilde{B}_\omega = \sqrt{\frac{\Lambda}{\omega}} \times \frac{1}{2c_0\sqrt{c_d}} \sqrt{\frac{c_u+v_u}{c_u-v_u}} \frac{\left(v_d^2-c_d^2\right)^{3/4}}{\left[c_u^2-c_d^2+c_u(v_u-v_d/\eta)\right]} \times \left[\sqrt{c_u^2-v_u^2}\left(c_u - c_d\frac{c_u/\eta+v_d}{c_u+v_u}\right) - i\sqrt{v_d^2-c_d^2}\left(c_u\frac{c_d\eta+v_u}{c_d+v_d} - c_d\right)\right]. \tag{B17}$$

Using our parameterization of the velocity profile given in Eqs. (8) and (9)

$$c_u = c_0\left[1+(1-q)D\right], \qquad v_u = -c_0(1-q\,D), \tag{B18}$$

$$c_d = c_0\left[1-(1-q)D\right], \qquad v_d = -c_0(1+q\,D), \tag{B19}$$

in the limit of small D, we obtain Eqs. (14) and (20).

Appendix C: Asymmetric profiles

In this Appendix we show that the results obtained in the main body of the text are still valid when considering flow profiles that generalize Eq. (9):

$$\frac{w_\alpha(x)}{c_0} = D\left[\alpha + \tanh\left(\frac{\kappa x}{c_0 D}\right)\right]. \tag{C1}$$

The parameter α fixes the asymmetry between the sub and supersonic flows with respect to the sonic horizon. This horizon exists only if $|\alpha|<1$, and it is located at

$$x_{\rm H} = -\frac{Dc_0}{\kappa}\,\mathrm{arctanh}(\alpha). \tag{C2}$$

The Hawking temperature corresponding to the velocity profile of Eq. (C1) is $T_{\rm H} = \kappa_\alpha/2\pi$, where

$$\kappa_\alpha \equiv \partial_x w_\alpha|_{x=x_H} = \kappa\left[1-\alpha^2\right]. \tag{C3}$$

In [16], we showed that when $|\alpha|<1$, the spectrum remains Planckian at low frequencies with temperature $T_{\rm H}=\kappa_\alpha/2\pi$ until ω approaches $\omega_{\rm max}$, where it vanishes. However, in the limit $|\alpha|\to 1$, $\kappa_\alpha\to 0$ and deviations from Planckianity appear at lower and lower frequency. Then, for $\alpha>1$, the flow is everywhere subsonic and there is no particle production because there are no negative norm modes with $\omega>0$. On the contrary, when $\alpha<-1$, the flow is everywhere supersonic. A new critical frequency $\omega_{\rm min}<\omega_{\rm max}$ appears, such that, for $0<\omega<\omega_{\rm min}$, there now exist 4 asymptotic in and out modes, two of them with positive norm and two with negative norm. Particle production will thus occur without sonic horizon, but the spectrum no longer diverges as $1/\omega$ for $\omega\to 0$.

Here we consider only the case where the horizon is present ($|\alpha|<1$), such that the effective temperature $T_{\rm eff}$ is well defined for $\omega\to 0$. The step-like analysis can be generalized to this situation, yielding (see Eq. (15))

$$T_{\rm step} = \frac{3\sqrt{3}}{8}\,\omega_{\rm max}(1+\alpha) \times \left[1-\left(q-\frac{1}{6}\right)(1-\alpha)D + O\left(D^2\right)\right], \tag{C4}$$

where $\omega_{\rm max}$ is obtained from Eq. (12) through the replacement $D\mapsto D(1-\alpha)$. Analogously one can compute the effective temperature of leftgoing particles

$$T^v_{\rm step} = \frac{3\sqrt{3}}{2}\,\omega_{\rm max}(1+\alpha)\,D^2\left(q-\frac{1}{2}\right)^2 \times \left[1-\left(q-\frac{1}{6}\right)(1-\alpha)D + \alpha\,\frac{2q^2-2q+1}{2q-1}\,\frac{D}{2} + O\left(D^2\right)\right]. \tag{C5}$$

Since the first term in the expansions of $T^v_{\rm step}$ have the same dependence on α as the first term of $T_{\rm step}$, their ratio

$$R_{\rm step} = 4\left(q-\frac{1}{2}\right)^2 D^2\left[1+\alpha\,\frac{2q^2-2q+1}{2q-1}\,\frac{D}{2}\right] + O\left(D^4\right) \tag{C6}$$

does not depend on α for small values of D.

In Fig. 8, $T_{\rm eff}/T_{\rm H}$ and $T_{\rm eff}/T_{\rm step}$ are plotted for a velocity profile with $\alpha=-0.5$. Nothing qualitatively changes in these plots with respect to the simpler case with $\alpha=0$. Even if α is relevant in determining the temperature of the emitted spectrum both in the Hawking and the step-like regime, the transition between them is still governed by $\omega_{\rm max}$ exactly as for $\alpha=0$. Thus it is again insensitive to the value of Λ/κ. We have extended our study for values of α closer than -1, and we observed no significant change.

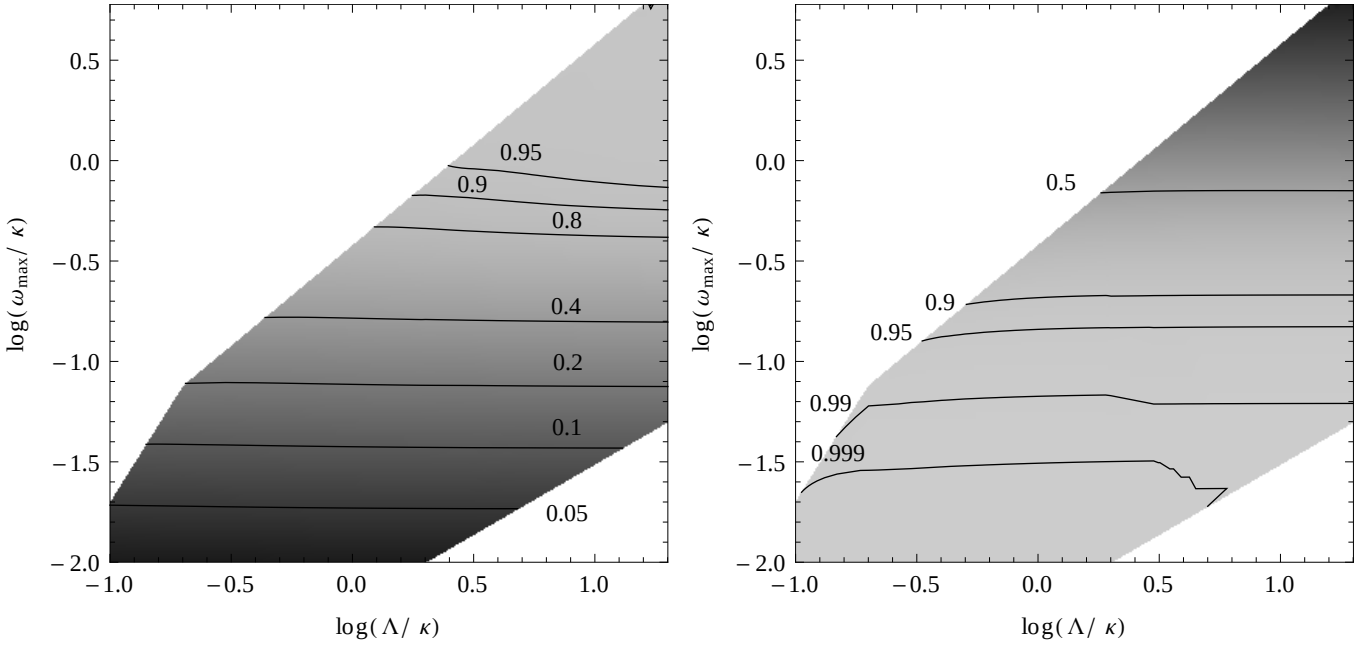

FIG. 8: $T_{\rm eff}/T_{\rm H}$ (left panel) and $T_{\rm eff}/T_{\rm step}$ (right panel) as functions of $\Lambda/\omega_{\rm max}$ and $\omega_{\rm max}/\kappa$ evaluated in the asymmetric flow profile of Eq. (C1) for $\alpha = -0.5$. The validity domains of both the Hawking and the step-like regime are not affected by the introduction of the parameter α which governs the asymmetry of the sub and supersonic regions.

[1] W. G. Unruh, Phys. Rev. Lett. **46**, 1351 (1981).
[2] W. G. Unruh, Phys. Rev. D **15**, 365 (1977).
[3] T. Jacobson, Phys. Rev. D **44**, 1731 (1991).
[4] T. Jacobson, Phys. Rev. D **48**, 728 (1993).
[5] R. Brout, S. Massar, R. Parentani, and P. Spindel, Phys. Rept. **260**, 329 (1995).
[6] W. G. Unruh, Phys. Rev. D **51**, 2827 (1995).
[7] R. Brout, S. Massar, R. Parentani, and P. Spindel, Phys. Rev. D **52**, 4559 (1995).
[8] S. Corley and T. Jacobson, Phys. Rev. D **54**, 1568 (1996).
[9] S. Corley, Phys. Rev. D **57**, 6280 (1998).
[10] Y. Himemoto and T. Tanaka, Phys. Rev. D **61**, 064004 (2000).
[11] W. G. Unruh and R. Schutzhold, Phys. Rev. D **71**, 024028 (2005).
[12] R. Balbinot, A. Fabbri, S. Fagnocchi, and R. Parentani, Riv. Nuovo Cim. **28**, 1 (2005).
[13] J. Macher and R. Parentani, Phys. Rev. D **79**, 124008 (2009).
[14] J. Macher and R. Parentani, Phys. Rev. A **80**, 043601 (2009).
[15] S. Finazzi and R. Parentani, Phys. Rev. D **83**, 084010 (2011).
[16] S. Finazzi and R. Parentani, Journal of Physics Conference Series **314**, 012030 (2011).
[17] A. Coutant, R. Parentani, and S. Finazzi, Phys. Rev. D **85**, 024021 (2012).
[18] A. Recati, N. Pavloff, and I. Carusotto, Phys. Rev. A **80**, 043603 (2009), 0907.4305.
[19] C. Mayoral, A. Fabbri, and M. Rinaldi, Phys. Rev. D **83**, 124047 (2011).
[20] S. J. Robertson, *PhD Thesis. Hawking Radiation in Dispersive Media* (2011), arXiv:1106.1805 [gr-qc].
[21] T. Jacobson and A. C. Wall, Foundations of Physics **40**, 1076 (2010).
[22] T. Jacobson and D. Mattingly, Phys. Rev. D **64**, 024028 (2001), arXiv:gr-qc/0007031.
[23] R. Parentani, Phys. Rev. D **63**, 041503 (2001), arXiv:gr-qc/0009011.
[24] P. Hořava, Phys. Rev. D **79**, 084008 (2009), 0901.3775.
[25] D. Blas and S. Sibiryakov, Phys. Rev. D **84**, 124043 (2011), 1110.2195.
[26] C. Barcelo, S. Liberati, and M. Visser, Living Rev. Rel. **14**, 3 (2011).
[27] C. W. Misner, K. S. Thorne, and J. A. Wheeler, *Gravitation* (W.H. Freeman and Co., San Francisco, 1973).
[28] R. Parentani, PoS **QG-PH**, 031 (2007).
[29] F. Dalfovo, S. Giorgini, L. P. Pitaevskii, and S. Stringari, Rev. Mod. Phys. **71**, 463 (1999).
[30] S. Weinfurtner, E. W. Tedford, M. C. J. Penrice, W. G. Unruh, and G. A. Lawrence, Phys. Rev. Lett. **106**, 021302 (2011).
[31] T. G. Philbin, C. Kuklewicz, S. Robertson, S. Hill, F. Konig, et al., Science **319**, 1367 (2008), 0711.4796.
[32] F. Belgiorno, S. L. Cacciatori, M. Clerici, V. Gorini, G. Ortenzi, L. Rizzi, E. Rubino, V. G. Sala, and D. Faccio, Phys. Rev. Lett. **105**, 203901 (2010).
[33] O. Lahav, A. Itah, A. Blumkin, C. Gordon, S. Rinott, A. Zayats, and J. Steinhauer, Phys. Rev. Lett. **105**, 240401 (2010).